Attack transients in clarinet models with different complexity - a comparative view

André Almeida, Baptiste Bergeot, C Vergez

Attack transients in clarinet models with different complexity - a comparative view

A. Almeida[a], B. Bergeot[b] and C. Vergez[c]
[a]School of Physics, University of New South Wales, 2052 Sydney, Australia
[b]LMA - CNRS UPR 7051, Aix-Marseille Univ., Centrale Marseille, 13402 Marseille, France
[c]LMA - CNRS, 31, chemin Joseph Aiguier, 13009 Marseille, France
andre.almeida@univ-lemans.fr

Recent works on simplified clarinet models using results from dynamic bifurcation theory have allowed to predict the evolution of the amplitude of sound (the amplitude envelope) for a gradual increase of the blowing pressure. The unrealistic model that predicted the amplitudes to attain very small values, far below the precision of a computer, was later corrected by the addition of stochastic noise to the model. The two models are useful in explaining and understanding why the oscillations appear with a delay relative to the threshold of oscillation that is predicted by purely steady-state models.
Both the model of the instrument and that of the noise are extremely simplistic, raising the question of its applicability to real instruments. These models can however be made gradually more complex by introducing more realistic details in the reed or in the resonator, and applying parameter profiles with more complex shapes or noise amplitudes. This presentation shows the differences encountered in the time-evolution of the acoustic wave simulated using two models of different complexity, one with an instantaneous reflection function, another with dispersion. The article explores to which extent can the dynamic predictive model be used to describe the time evolution of more realistic models, and hopefully that of the real instrument.

1 Introduction

Raman's model [1], typically used for bowed instruments, can also be extended to reed instruments, providing a simplified model for the clarinet [2] that is more easily understandable than other more complex models. It has provided insight in the determination of oscillation amplitudes and thresholds of oscillation [3] and more recently, oscillation thresholds in for variable parameters in undisturbed [4] or noisy [5] conditions. In these two later works, one of the questions that remains unanswered is how the predictions of this simplified model compares to more complex models that include details such as a more realistic bore, or reed dynamics. This article aims at providing some insight into this problem, by comparing results obtained with Raman's model with slightly more complex models that include some dispersion in the wave propagation in the bore. In a first stage reed dynamics is not yet included.

1.1 The Model

Raman's model supposes that the incoming wave arriving at the reed is an exact but inverted copy of the outgoing wave, and further multiplied by a factor smaller or equal to unity. In practice this insures that the signal generated by the model is a square wave. The propagation and reflection in the bore can thus be considered as generating an incoming presure wave p^- by the convolution of an outgoing pressure wave p^+ with a reflection function that is simply a Dirac distribution $\delta(t-T)$:

$$p^-(t) = p^+(t) * r(t) = p^+(t) * (-\delta(t-T)) = -p^+(t-T) \quad (1)$$

Here, T is the time taken by a roud-trip in the bore.

In a straight resonator, the reflection function is a rather sharp peak that quickly approaches 0 for the values of the delay τ far from the propagtion time [6]. It is different from a Dirac distribution, which has an infinitesimal width. A real reflection function is usually non-symmetric around its maximum. However, since the present model is still simulated in discrete-time, a non-symmetrical reflection function can easily lead to a period that corresponds to a fractional number of samples. Although it is possible to design a reflection function that leads to an integer number of samples, this case will be dealt with in the future.

The model studied in this article replaces the impulse reflection function by a spread-out reflection function. For simplicity, the reflection function is symmetrical, so that the period of the generated signal $(2 * T)$ can be easily compared to that of the original Raman's model. Such a function does not have physical meaning, but very roughly reproduces the effect of a low-pass filter which also exists in a straight tube.

Simulations are ran at a higher precision than machine double precision, with 200 decimal digits. For this purpose, a *python* library (*mpmath*) is used. In variable blowing pressure simulations with rates of increase of the blowing pressure of 0.001 and 0.01, 200 decimals is aprroximately the minimum precision at which round-off errors are negligible [4].

2 Steady state results

For a first analysis, the simulations are performed at 8 samples per round-trip, that is, the delay corresponding to a round-trip in the resonator corresponds to 8 samples. The analysis consists in comparing two simple reflection functions. The first one corresponds to a Dirac, giving the same results as the iterated map provided that the initial condition is given by a vector of 8 identical samples. The second reflection function is a "rectangular" function with a variable width w samples (Rect_w). Instead of being a copy of the outgoing wave, the incoming wave is now an average of w samples of the outgoing wave, so that a step transition is reflected as a smoothed-out transition. In practice any real reflection function acts as a filter. The rectangular function is then a low-pass filter. The two functions are scaled such that the sum of all samples is the same, as shown in figure 1 for a width $w = 3$ samples.

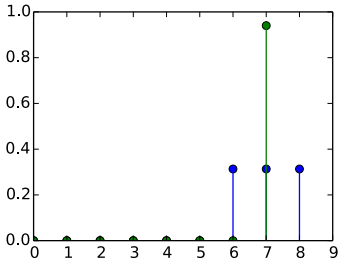

Figure 1: Reflection functions used in the examples below: dirac delta in green and Rect_3 in blue

A simulation ran at $\gamma = 0.8$, $\zeta = 0.5$, but an exaggerated value of losses (fig. 2, with $\lambda = 0.85$ vs. typically $\lambda \simeq 0.95$ for the full length of the clarinet resonator [7]) shows that, although the shape of the permanent regime (or equivalently

the harmonic decomposition) is quite different in the two systems, their peak amplitudes match quite closely.

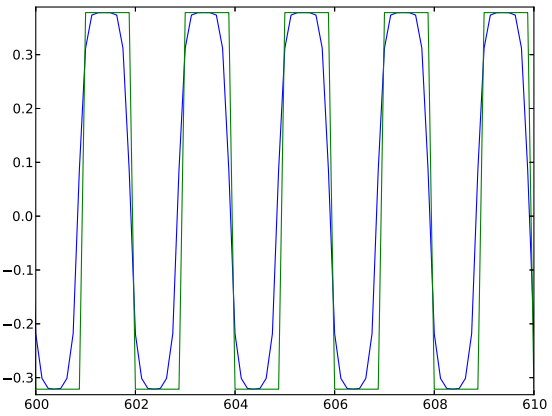

Figure 2: Steady-state regime: comparison of an instantaneous reflection function and a "Rectangular" reflection function of width 3 (Rect_3).

Even if the parameters are maintained constant throughout the simulation, in practice there is a transient at the beginning of the simulation, because the initial conditions do not match the permanent regime. For the same values of the parameter, the initial transient is represented in figure 3. Once more, the time-evolution of the amplitudes, or their envelope seems to match in the two cases.

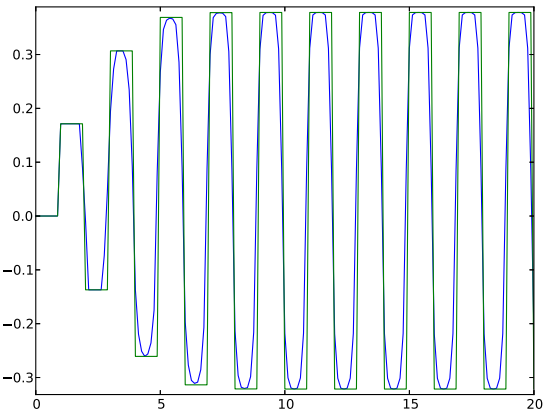

Figure 3: Transient regime: comparison of the two cases shown in figure 2

The agreement between the amplitudes can seem natural: in fact, if for a fraction of the period that is long enough the pressure remains almost constant (which is observed in pressure signals measured inside the resonator at particular notes), the averaging performed by the reflection function may act on values of pressure that are almost the same, producing the same amplitude as if they were convoluted by a dirac function. However, further examples show that this is not always the case.

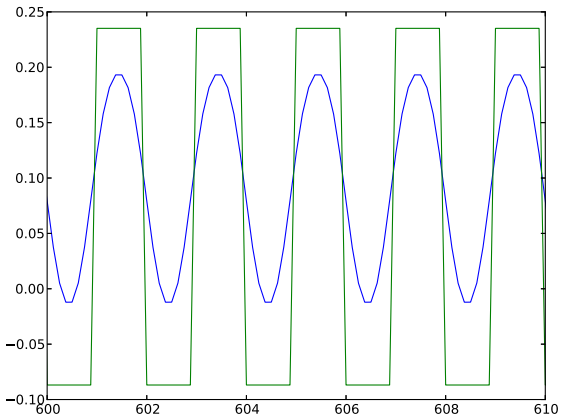

Figure 4: Steady-state regime: comparison of an instantaneous reflection function and a "rectangular" reflection function of width 3.

2.1 Significant differences between reflection functions

Figure 4 shows a simulation similar to the previous section, but with a lower value of $\gamma = 0.45$. In this case the waveforms are totally different, and this has consequences in their amplitude, as it is not possible to consider that there is an almost constant plateau in each period.

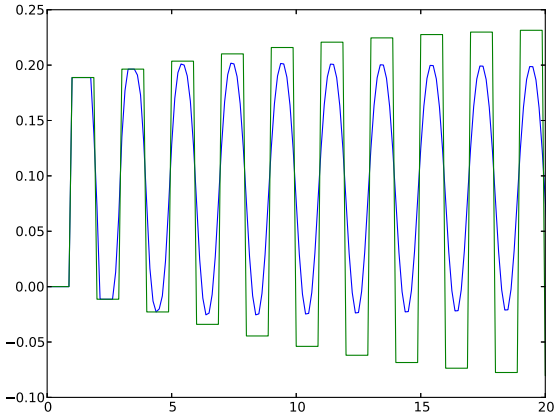

Figure 5: Transient: comparison of an instantaneous reflection function and a "rectangular" reflection function of width 3. (same parameters as in figure 4)

In fact, the situation is less dramatic on the starting transient (fig. 5), because in the beginning the waveform is closer to a square wave. After a few reflections, the smoothing effect is too heavy, so that the higher harmonics are almost absent and the wavefrom is almost sinusoidal.

It should be noticed that there are two effects working in opposite directions. The rectangular reflection function acts as a low-pass filter, and successive reflections tend to bring the waveform close to a sinusoid. The non-linearity (which can be thought of as a "non-linear instantaneous reflection" at the extremity of the mouthpiece) is enriching the harmonic content of the waveform. In fact, if the reflection at the extremity of the mouthpiece were a passive reflection, the waveform would eventually become sinusoidal in all cases.

3 Variations in the parameter space

3.1 Periodicity in parameter space

Figure 6 shows how the regions of period doubling remain almost constant in both the dirac reflection and the smoother reflection with a square function of 3 samples (within a round-trip time of 8 samples). The graphics show a simulation ran at $\lambda = 0.95$ and variable γ on the horizontal axis and ζ on the vertical axis.

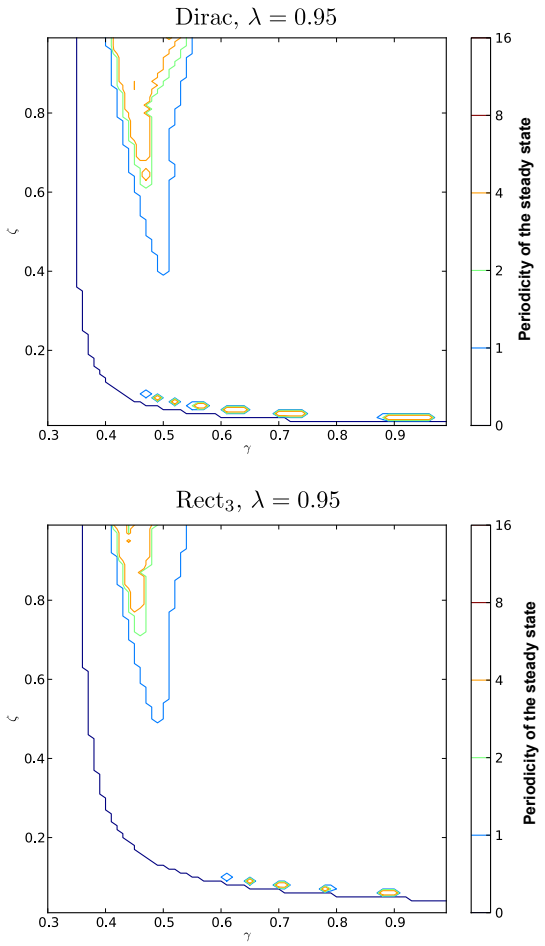

Figure 6: Limits of the regions with different periodicities: on the left and bottom, the time-series converges to a constant value. On most of the parameter-space, the time series has a period 1 (two round trips), and in the top regions of increasing periodicity are seen.

3.2 Amplitude in the parameter space

A similar conclusion can be drawn for the amplitude of the steady state, as shown in figure 7. In this figure, the amplitude is calculated from the RMS value of a period in the end of the simulation. Although not shown here, the amplitudes of the first harmonic show similar results, although with a scaling factor. Peak amplitudes show slightly different results.

The parameter space maps show that although a particular set of parameters produce different behaviour, in particular different amplitudes of oscillation, these are rather localised effects when looking at peak-to-peak amplitudes. This reassuring conclusion, if confirmed in other more complex reflection functions, may mean that differences observed between models and experimental measurements [8] are not a consequence of the details of the resonator.

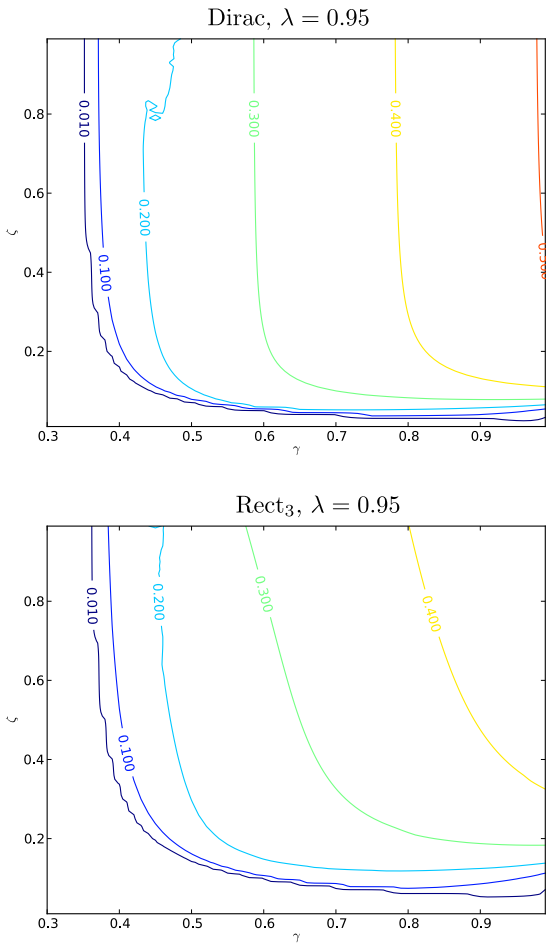

Figure 7: RMS amplitude contours in the parameter space.

3.3 Detail for constant parameters and variable γ

Figure 8 shows a cross-section of the map in figure 7 through a line of constant ζ. The peak amplitudes of oscillation are coincident in most of the range of γ, which correspond to the regime in which the reed is beating. In the non-beating region, up to approx 0.5, the situation is similar to that shown in figures 4 and 5.

However, figure 9 shows that the RMS amplitudes are always lower throughout the whole range of γ. This is as expected, since the RMS value of a square wave is always bigger than that of a different waveform with similar peak amplitude.

4 Transient times

There are multiple ways of defining the transient time, no consensus existing on a preferred one. In this section, we chose to define it as the time needed to reach a fraction of the final amplitude (see figure 10). Of course this definition should work reasonably well for signals generated in a simulation, as in this work, and introduce some problems with real signals.

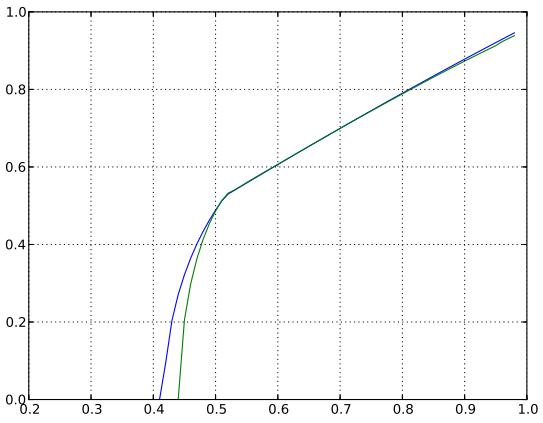

Figure 8: Peak amplitudes of the steady state as a function of parameter γ. $\lambda = 0.85$

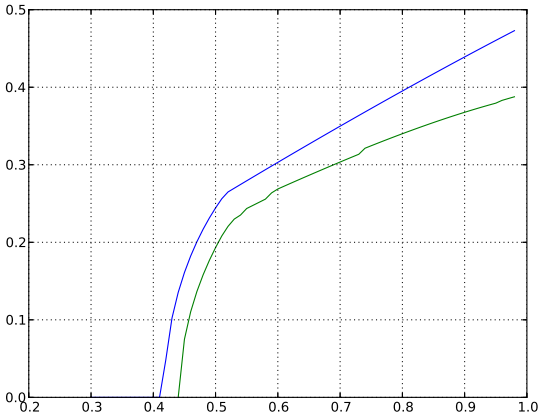

Figure 9: RMS amplitudes of the steady state as a function of parameter γ. $\lambda = 0.85$

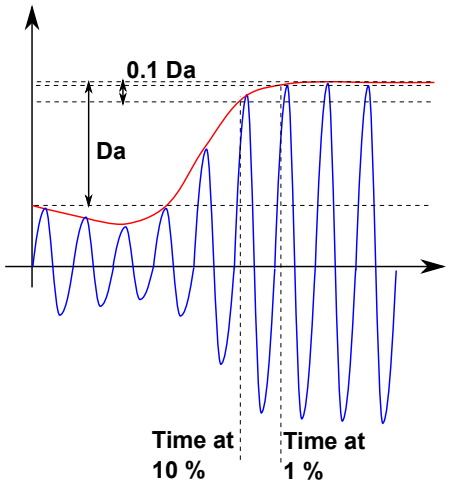

Figure 10: Method of estimating transient times

Defined this way the transient times at 0.1% (1/1000 of the total amplitude change) are shown in figure 11.

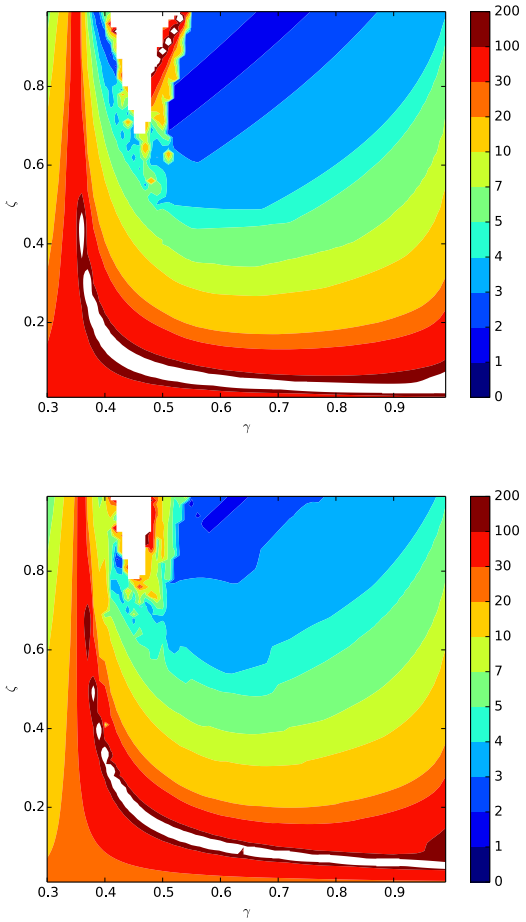

Figure 11: Contours of equal time to arrive at an amplitude which is nearer than 10% of the final amplitude. Top: dirac reflection function, bottom: Rect_3 reflection function. Color scale is in number of round-trips.

5 Variable parameter γ

This section investigates the changes in sound envelopes for variable blowing pressures (parameter γ). In particular, one of the aims is to check whether oscillations can appear at significantly different times when the reflection function is not an impulse. The same principle is used as before, however there is an important detail on how the growing parameter is defined when multiple samples per round-trip are used. In order that the system is similar to the one sample per round, the input mouth pressure must not vary within that round trip. Instead of having a linearly increasing mouth pressure, the input signal resembles a stepped function.

The definition of transient time is now changed from the previous section. Since the parameter γ does not stop increasing, the same happens to the oscillation amplitude (see for instance, the top graphic in figure 12. For this reason, and because the main delay is the waiting time until the oscillations appear (the "dynamic oscillation threshold"), the transient time is now defined as the number of round-trips until the amplitude reaches a constant value, 0.1 in this case.

With variable parameter, the non-instantaneous reflection function seems to always show longer delays than the Dirac. A typical comparative result with the two reflection functions (dirac impulse and square reflection function) is represented in figure 12, both in terms of envelope (peak-to-peak) and a

detail of the time signals at the dynamic oscillation threshold.

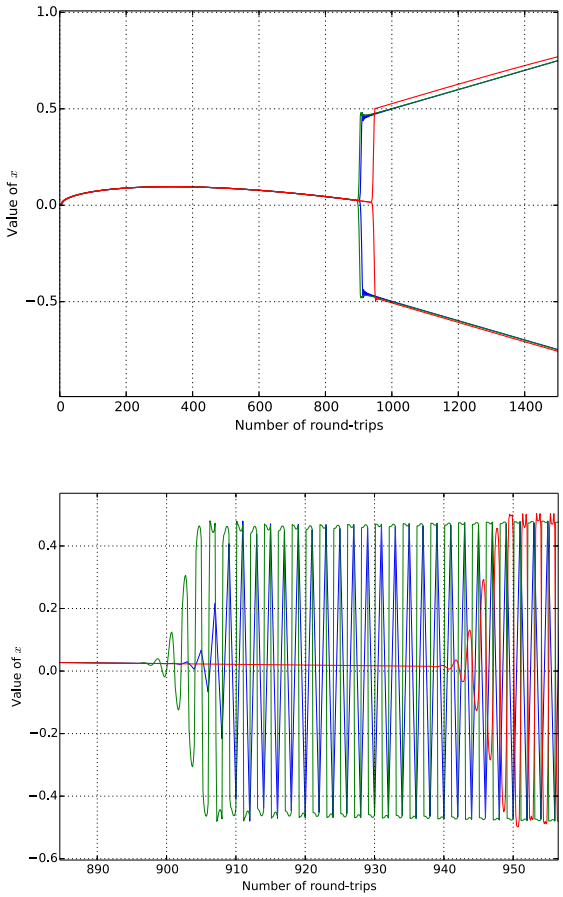

Figure 12: Comparison of three simulations with similar parameters but different reflection functions (top: envelopes, bottom: time signal in the vicinity of the bifurcation; blue: one sample per round-trip, green: dirac reflection, red: square reflection function with a width of 3 samples on 8 samples per round-trip, other parameters are constant $\Delta\gamma = 1/1000$, $\zeta = 0.5$, $\lambda = 1$).

This may be explained by a higher effective loss parameter (λ) for the square reflection function. In fact, in small oscillations only the f_0 component exists, so that only the first peak of the reflection function (corresponding to the first impedance peak) contributes to the exponential growth.

Overal, in a significant part of the parameter space ζ, λ (the embouchure parameter, and the amount of losses in the acoustic resonator), oscillations are produced in the case of an instantaneous (dirac) reflection function, whereas no oscillations arise in the case of the rectangular (Rect_3) reflection function. These are shown in white in figures 13 and 14 for two different rates of increase of the parameter γ (the blowing pressure).

Only for stronger lip forces and small acoustic losses does the rectangular reflection function produce oscillations (typically with similar peak amplitudes, as in the case of steady blowing pressures, sect. 3.2). In general, these arise later than in the case of the instantaneous reflection function, but bigger lip forces produce smaller relative delays.

The case of faster increasing pressures is harder to analyse (fig. 14). In general, the relative delays are comparable to the slower rates of figure 13 if we take into account that for example during 2 round-trips of the faster

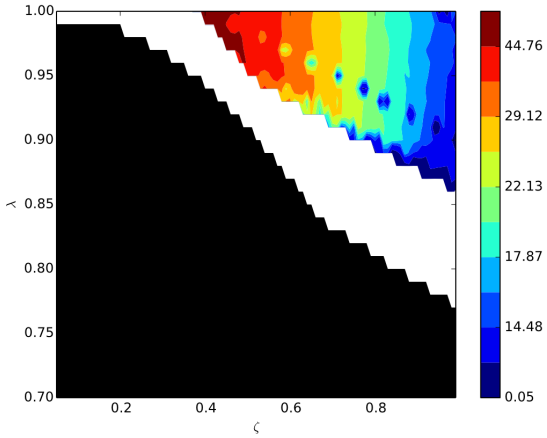

Figure 13: Number of samples between the appearance of oscillation for a Dirac impulse reflection function and for a square reflection function 3 samples wide. In the black region no oscillation exists in both cases, in the white region only the system with a Dirac reflection oscillates. Mouth pressure γ increases at a rate of 1/1000 per round trip.

rate, parameter γ increases as much as during 20 round-trips of the slower rate. However, in a significant region of the parameter space, very large relative delays arise.

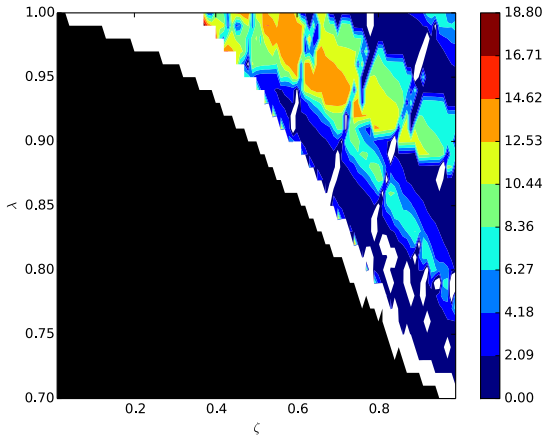

Figure 14: Number of samples between the appearance of oscillation for a Dirac impulse reflection function and for a square reflection function 3 samples wide. In the black region no oscillation exists in both cases, in the white region only the system with a Dirac reflection oscillates. Mouth pressure γ increases at a rate of 1/1000 per round trip.

6 Conclusions

The few demonstrations presented in this article are an overview of differences in behaviour between "equivalent" self-oscillating systems with the only difference in the reflection function. It was shown that in many cases the characteristics of the steady state oscillation are mostly independent of the reflection function, at least for the two functions that were tested. There are however some important differences when the parameters vary slowly through time: when the reflection function is not

instantaneous (i.e. it is a function with finite time support instead of a dirac impulse) the duration of the transient is slightly longer. In some cases the oscillation cannot be maintained in similar conditions (same playing parameters and reflection coefficient). These results will help to explain the behavior of clarinet instruments when measured in controlled increases of the blowing pressure [9].

References

[1] C. V. Raman. On the mechanical theory of vibrations of bowed string [etc.]. *Assoc. Cult. Sci. Bull.*, 15:1–158, 1918.

[2] S. Ollivier, J. P. Dalmont, and J. Kergomard. Idealized models of reed woodwinds. part 1 : Analogy with bowed string. *Acta. Acust. Acust.*, 90:1192–1203, 2004.

[3] J. P. Dalmont and C. Frappe. Oscillation and extinction thresholds of the clarinet: Comparison of analytical results and experiments. *J. Acoust. Soc. Am.*, 122(2):1173–1179, 2007.

[4] B. Bergeot, C. Vergez, A. Almeida, and B. Gazengel. Prediction of the dynamic oscillation threshold in a clarinet model with a linearly increasing blowing pressure. *Nonlinear Dynam.*, 73(1-2):521–534, 2013.

[5] B. Bergeot, C. Vergez, A. Almeida, and B. Gazengel. Prediction of the dynamic oscillation threshold in a clarinet model with a linearly increasing blowing pressure: Influence of noise. *Nonlinear Dynam.*, 74(3):591–605, 2013.

[6] R. T. Schumacher. Ab initio calculations of the oscillations of a clarinet. *Acustica*, 48:71–85, 1981.

[7] A. Chaigne and J. Kergomard. Instruments à anche. In *Acoustique des instruments de musique*, chapter 9, pages 400–468. Belin, 2008.

[8] Andre Almeida, David George, John Smith, and Joe Wolfe. The clarinet: How blowing pressure, lip force, lip position and reed "hardness" affect pitch, sound level, and spectrum. *The Journal of the Acoustical Society of America*, 134(3):2247–2255, 2013.

[9] B. Bergeot, A. Almeida, B. Gazengel, C. Vergez, and D. Ferrand. Response of an artificially blown clarinet to different blowing pressure profiles. *J. Acoust. Soc. Am.*, 135(1):479–490, 2014.